JOURNAL OF AIRCRAFT
Vol. 32, No. 6, November–December 1995

Computational Inlet-Fairing Effects and Plume Characterization on a Hypersonic Powered Model

Lawrence D. Huebner*
NASA Langley Research Center, Hampton, Virginia 23681-0001

A three-dimensional computational study has been performed addressing issues related to the wind-tunnel testing of a hypersonic powered-simulation model. The study consisted of two related objectives. The first objective was to determine the three-dimensional flow effects on the aftbody created by fairing over the inlet; this was accomplished by comparing the computational fluid dynamics solutions of two closed-inlet powered configurations with a flowing-inlet powered configuration. Results at four freestream Mach numbers indicate that the exhaust plume tends to isolate the aftbody surface from most forebody flowfield differences, a smooth inlet fairing provides the least aftbody force and moment variation compared to a flowing inlet. The second objective was to predict and understand the three-dimensional characteristics of exhaust plume development at selected points on a representative flight path of a single-stage-to-orbit vehicle. Results showed a dramatic effect of plume expansion onto the wings as the freestream Mach number and corresponding nozzle pressure ratio are increased.

Nomenclature

M	=	Mach number
NPR	=	nozzle pressure ratio, $p_{t,\text{jet}}/p_\infty$
p	=	pressure, Pa
Re	=	Reynolds number, 1/m
T	=	temperature, K
α	=	angle of attack, deg
ΔM	=	Mach number increment, see Figs. 3–5
ρ	=	density, kg/m^3

Subscripts

throat	=	conditions at the internal nozzle throat
t, jet	=	jet total conditions
wall	=	conditions at a solid wall boundary
∞	=	freestream conditions

Introduction

RESEARCH performed on single-stage-to-orbit (SSTO) vehicles like the National Aerospace Plane (NASP) requires accurate determination of the aeropropulsive effects and performance of hypersonic airbreathing configurations under powered conditions. To accomplish this, a wind-tunnel model is typically designed and fabricated with some method of simulating the powered effects of scramjet combustion. One such method uses a noncombusting gas to simulate some of the major scramjet exhaust properties. This simulant gas is routed from an external supply and through the model support structure (strut or sting) to the model. The exhaust flow is then established in the plenum chamber of the model and expanded over the aftbody through an appropriately-designed nozzle.

Two methods of treating the inlet flow are to ingest the flow into the inlet or to design a geometrical inlet fairing to divert the oncoming inlet flow around the inlet plane. Due to the relatively small scale of model that can be tested in typical hypersonic wind tunnels, as well as the short engine-module lengths employed on these models, it is impractical to use the flow-ingesting method, which requires both capturing the inlet flow and producing the simulated exhaust flow. There is simply not enough volume to process both the inlet and exhaust flow. The inlet flow would have to either pass directly through the model or be evacuated out of the model. The second approach for treating the inlet flow is to employ a fairing from the forebody to the cowl leading edge and divert the inlet flow around the outside of the model. However, such forebody geometry changes affect the flowfield structure in the forebody region and may affect the aftbody/exhaust interactions as well.

This computational study consists of two related parts. The first objective is to determine the three-dimensional effects of inlet fairing on the aftbody. The inlet-fairing study is an attempt to ascertain the influence of these nonrealistic (but necessary for wind-tunnel testing) forebody configurations on the powered aftbody and wings for four different freestream Mach numbers and associated nozzle pressure ratios. The second objective is to predict and understand the three-dimensional characteristics of exhaust plume development at selected points on a SSTO vehicle representative flight path. An understanding of the extent of the plume boundaries for a series of freestream Mach numbers and nozzle pressure ratios is presented.

Computational Code

The objectives of this study were performed using the General Aerodynamic Simulation Program (GASP).[1,2] GASP solves the integral form of the Reynolds-averaged Navier–Stokes equations and its subsets, namely, the Euler, parabolized Navier–Stokes (PNS), and thin-layer Navier–Stokes (TLNS) equations. GASP is a fully three-dimensional code employing structured multiblock grids, mesh sequencing, and a variety of computational, transport, thermodynamic, and chemistry models.

Inlet-Fairing/Plume Studies

Before any computational fluid dynamics (CFD) code can be used as an analysis tool, code calibration is essential for the types of flows of interest to provide a level of confidence

Presented as Paper 93-3041 at the AIAA 24th Fluid Dynamics Conference, Orlando, FL, July 6–9, 1993; received Sept. 26, 1993; revision received March 27, 1995; accepted for publication May 15, 1995.

*Aerospace Engineer, Hypersonic Airbreathing Propulsion Branch, Gas Dynamics Division, M/S 168. Senior Member AIAA.

Table 1 Physical conditions for inlet-fairing/plume study

M_∞	3.40	5.92	10.14	13.66
Re_∞	6.56×10^6	6.56×10^6	6.56×10^6	6.56×10^6
NPR	30	200	3,000	40,000
T_∞, K	102.25	55.838	49.556	50.621
p_∞, Pa	1,982.05	474.773	209.531	174.267
ρ_∞, kg/m^3	6.756×10^{-2}	2.964×10^{-2}	1.474×10^{-2}	1.200×10^{-2}
M_{throat}	1.034	1.034	1.034	1.034
T_{throat}, K	329.934	329.934	383.337	708.611
p_{throat}, kPa	31.537	50.361	333.388	3,697.1
ρ_{throat}, kg/m^3	0.74344	1.18720	6.76431	40.5791

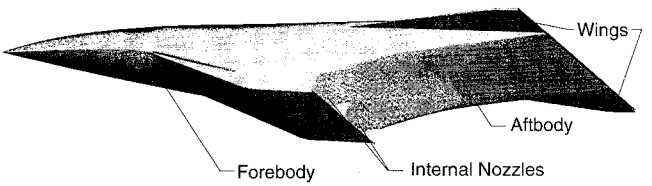

Fig. 1 Numerical surface of NASA Langley's TTD powered model configuration.

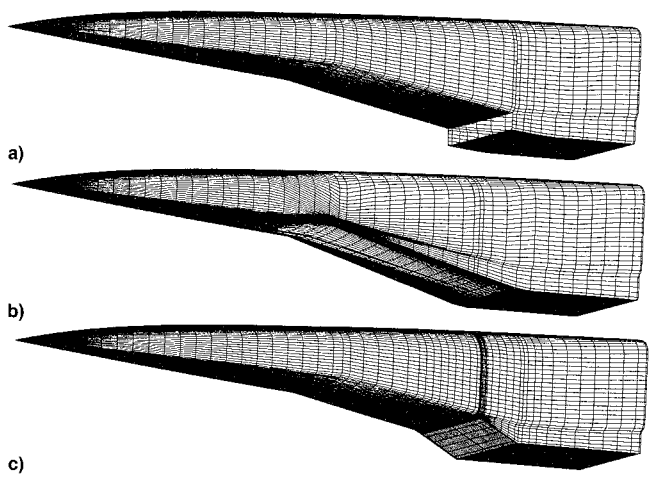

Fig. 2 Computational forebody surface representations: a) flow-ingested, b) faired-over, and c) blocked-off inlets.

in the ability of the code to accurately predict the fluid dynamics of the problem. Previous studies using GASP have shown that it has the ability to accurately predict complex three-dimensional hypersonic flows past configurations representative of NASP forebodies,[3–5] as well as two- and three-dimensional powered effects on model aftbodies.[6–8] Having gained some confidence in the code's ability to predict aftbody surface-pressure effects, the interest herein is to gain insight into the effects of inlet fairing and plume characteristics on the powered aftbody.

Geometry

The computational geometry used in this part of the study was the powered test technique demonstrator (TTD) model (Fig. 1). The geometry consists of three different forebody representations, an internal nozzle, and an aftbody including a wing at an incidence angle of -1.5 deg. The three different three-dimensional forebody/inlet representations of interest in the inlet-fairing/plume studies are shown in Fig. 2. The flow-ingested inlet model (Fig. 2a) represents the external geometric features of a flowing inlet and assumes that the inlet flow is completely captured (no spillage) and that the external flow beyond the cowl is not influenced by what occurs within the inlet. The last two representations can be categorized as closed-inlet configurations. The faired-over inlet (Fig. 2b) is a "soft" fairing, beginning at the compression ramp break of the forebody and developing along straight-line rays to the cowl leading edge. This was the initial attempt at minimizing the influence of the fairing on the plume and nozzle. The blocked-off inlet (Fig. 2c) is a "worst-case" fairing, produced by closing off the inlet with a planar surface between the forward extent of the engine sidewall leading edges. However, it is also of interest because it represents the typical unpowered vehicle entry configuration. The internal nozzle contour was varied to provide appropriate values of exhaust cowl-exit Mach number for each freestream Mach number. The aftbody with wings is identical for all simulations. Solutions were performed on a semispan model to conserve computational resources. The total number of computational cells for each of these configurations is about one million.

Physical Conditions for Computational Solutions

This computational procedure allowed for the prediction of external flow features for the three inlet representations without regard for the ingested "flow" into the inlet. The approach taken was to merge the flowfields computed from each of the three forebody/inlet representations with the same internal nozzle solution for each of four prescribed freestream Mach numbers. The resulting aftbody solutions then had both the primary plume influence near the body from the internal flow, as well as the differences in external flow resulting from the different forebodies. Each complete three-dimensional PNS solution simulating a powered model is composed of three parts. The external forebody and internal nozzle solutions were computed separately. Then flow information required by GASP to start the aftbody solution was obtained at cell centers of the aftbody grid at the cowl trailing edge using bilinear interpolation of the external forebody and internal nozzle flow variables computed at the cowl trailing edge.

The physical information necessary to generate solutions for the four different Mach numbers of interest is provided in Table 1. All cases were performed at $\alpha = 0$ deg. Freestream and nozzle throat conditions produce the four different representative nozzle pressure ratios (NPRs) for the four different freestream Mach numbers. As can be seen from the table, both the external freestream pressure and the internal jet total pressure variation with Mach number can be seen in the large extremes in NPR. For this study, the simulant exhaust gas is modeled as a single-species gas with a molecular weight equal to that of a CF_4Ar mixture used for noncombusting, scramjet-exhaust flow simulation.[9] The ratio of specific heats was fixed at 1.27, the approximate average value for the varying specific heat ratio in the aftbody region for the actual CF_4Ar mixture (which is thermally perfect).

CFD Solution Issues

The boundary layers for all solutions were assumed to be laminar. In the streamwise direction, full fluxes were employed using a Van Albeda-type smooth limiter and second-order, fully upwind spatial discretization. In the circumferential direction, Van Leer's flux vector splitting was used with the Spekraize–Venkat limiter and third-order, upwind-biased

spatial discretization. In the body-normal direction, Roe's flux difference splitting was used with the Spekraize–Venkat limiter and third-order, upwind-biased spatial discretization.[1] In addition to the prescribed initial conditions imposed on the first solution plane of the forebody and the internal nozzle grids, a no-slip, fixed-wall-temperature boundary condition was imposed on all body surfaces (T_{wall} = 305.33 K), while first-order extrapolation boundary conditions were imposed on the outer grid boundary. The downstream boundary was ascribed a second-order extrapolation boundary condition, while the upper and lower center-planes of the grid had an x-z symmetry boundary condition imposed. The grids were clustered near solid surfaces such that the average value of the inner law variable[10] at the first computational cell center away from the body was about 3, with some localized regions that were as high as 12 (on the wing leading edge). Marching plane residuals were reduced five orders of magnitude for the first three planes of the external and internal flows, providing a good establishment of the solution features. The remainder of the marching planes was converged to four orders of magnitude residual reduction since this was adequate to stabilize the surface pressures and other flowfield features of interest.[11] One additional issue was that some of the aftbody solutions were computationally stiff, particularly at the high NPRs, and required that the initial few planes be solved with first-order spatial accuracy in the streamwise direction and then recomputed using second-order spatial accuracy.

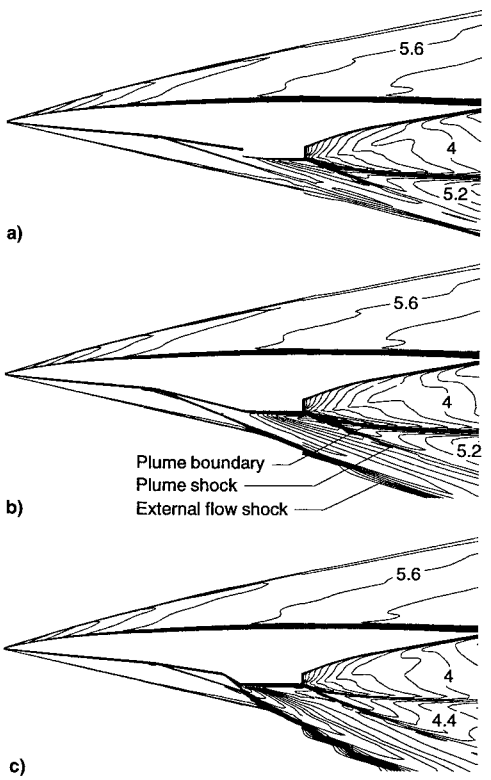

Fig. 3 Centerline Mach number contours, M_∞ = 5.92, NPR = 200 (ΔM = 0.2): a) flow-ingested, b) faired-over, and c) blocked-off inlets.

Inlet-Fairing Results

Results of the inlet-fairing study are presented with representative plots of Mach number contours at the model centerline and at aftbody cross-planes, aftbody lower surface pressure contours, and relative force and moment data. The flowfield plots are not inclusive of all solutions performed, but highlight the major physical phenomena that are caused by the different forebody representations. The force and moment data do include information from all solutions that were performed.

To illustrate the flowfield differences caused by the different forebody geometries, centerline Mach number comparisons are shown (Fig. 3) for the M_∞ = 5.92, NPR = 200 condition. As expected, the upper surface flow is unaffected by the variation in inlet representation. The effect of the stronger shocks from the faired-over and blocked-off inlet cases is evident when compared with the flow-ingested inlet solution. Note that, for the blocked-off inlet case, the intersection of the two forebody shocks, one from the compression ramp break and one from the beginning of the blocked inlet, is very near the cowl leading edge, behind which the flow rapidly expands over the surface of the cowl. Also, the cowl boundary layer for the flow-ingested inlet case is much smaller than the other two cases, since the boundary layer develops from the cowl leading edge, not the forebody nose as for the faired-over and blocked-off inlet cases. Small differences in Mach number contours within the plume shear layer can be seen, but the actual location of the shear layer is basically unaffected by the different forebody representations.

Comparisons of flowfield Mach number contours are presented for each of the three comparative CFD solutions at M_∞ = 5.92, NPR = 200 for locations just beyond the cowl trailing edge and at the body trailing edge in Figs. 4 and 5, respectively. In Fig. 4, flowfield differences are confined to the external flow, since the internal solutions were identical

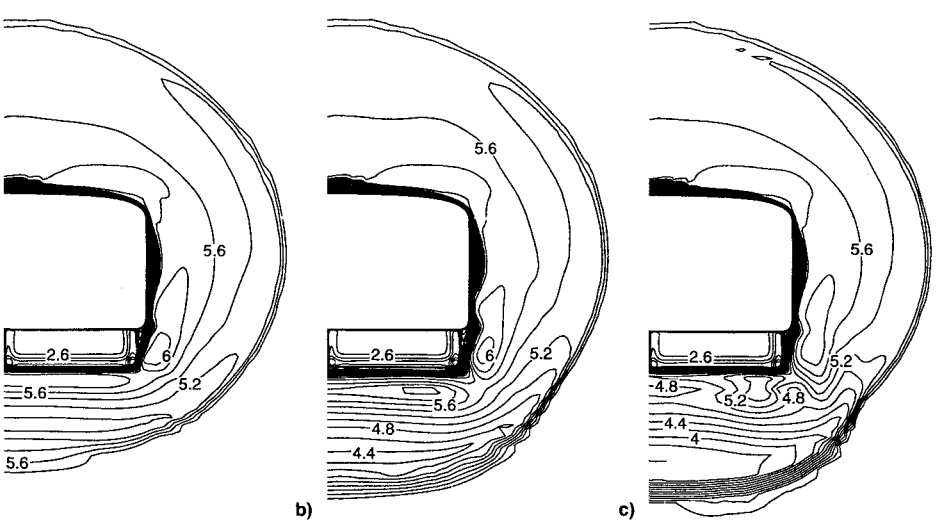

Fig. 4 Mach number comparisons, just beyond cowl trailing edge, M_∞ = 5.92, NPR = 200 (ΔM = 0.2): a) flow-ingested, b) faired-over, and c) blocked-off inlets.

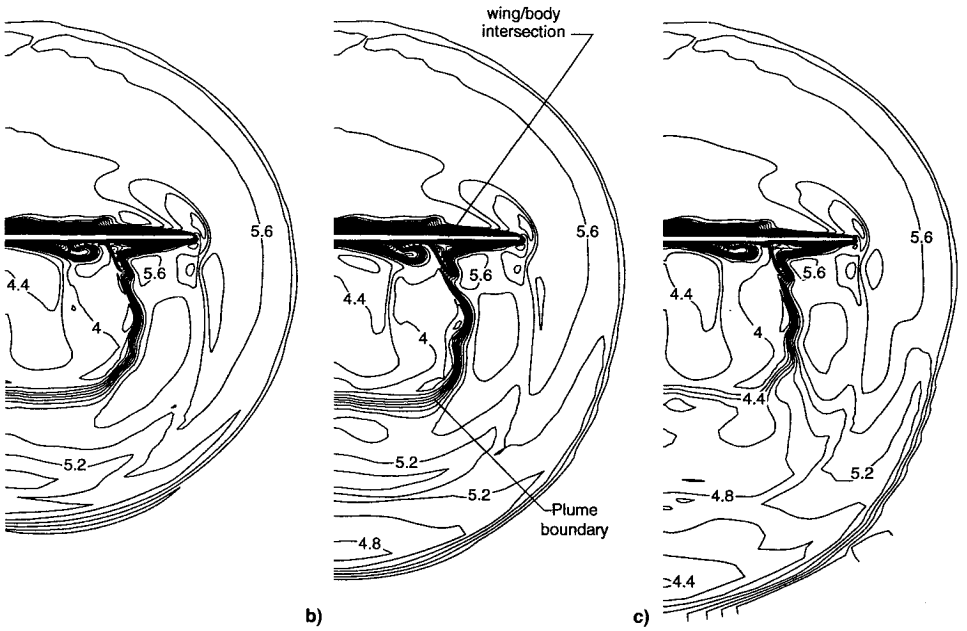

Fig. 5 Mach number comparisons, body trailing edge, M_∞ = 5.92, NPR = 200 (ΔM = 0.2): a) flow-ingested, b) faired-over, and c) blocked-off inlets.

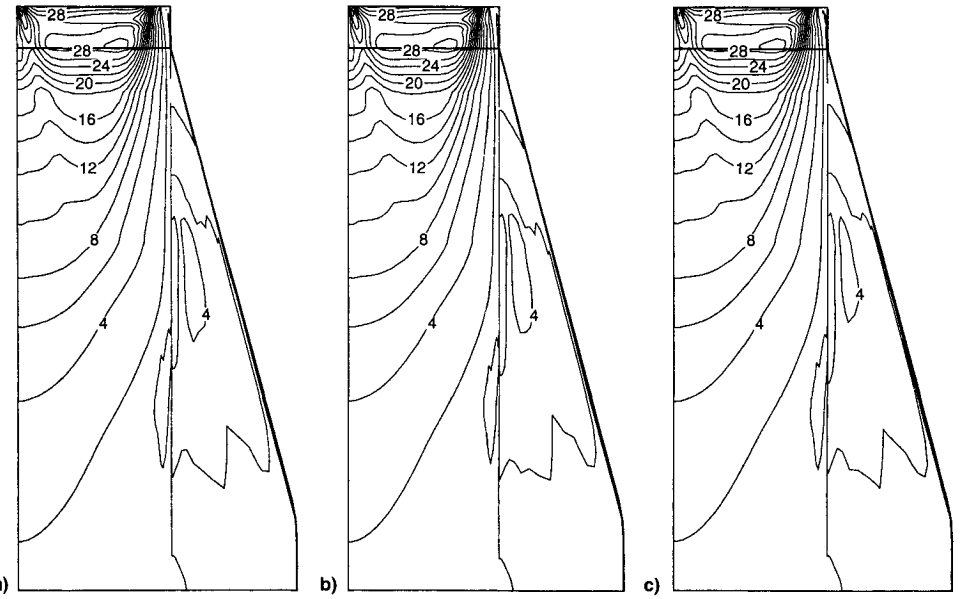

Fig. 6 Aftbody lower surface pressure comparisons (p/p_∞ contours), M_∞ = 10.14, NPR = 3000: a) flow-ingested, b) faired-over, and c) blocked-off inlets.

for each of the three solutions. The stronger shocks for the two closed-inlets (Fig. 4b and 4c) can be seen below the body, along with the fact that the flow between the external shock and the plume does not expand back to the same Mach number as the flow-ingested inlet solution. Furthermore, there is evidence of additional flow structure below the outboard lower corner of the cowl for the closed-inlet solutions generated by the oncoming flow being diverted around the closed-off inlets. Figure 5 shows that at this value of NPR the plume does not expand much out over the wings and maintains a nearly rectangular shape. The strength of the lower part of the shear layer is diminished for the blocked-off inlet as seen by fewer Mach number contours that make up the shear layer. However, the Mach number contours near the surface and the flow within the plume are nearly identical for the three cases including the complex plume/boundary-layer interaction near the wing/body intersection, indicating that the plume tends to isolate the aftbody lower surface from the external forebody flow features.

Comparisons of pressure contours on the lower surface of the aftbody and wing are shown in Fig. 6 for the M_∞ = 10.14, NPR = 3000 condition. (Results are similar for the other three Mach numbers.) Upper surface pressure contours on the aftbody were virtually identical for all three cases (and thus are not presented here), indicating that the effect of the plume is restricted to the lower surface for the conditions simulated. Figure 6 is presented as pressure ratio comparisons, where the local surface pressure has been normalized by the freestream pressure at this condition. Close examination of the two closed-inlet solutions shows only very small differences in pressure on the lower surface of the aftbody and wing compared with the flow-ingested inlet solution. Once again, plume isolation of the aftbody lower surface mitigates the effects of the flowfield differences outside of the plume.

Figure 7 presents the relative aftbody force and moment data as determined by pressure area integration on the aftbody, i.e., that part of the configuration downstream of the cowl trailing edge. Each part of Fig. 7 shows two kinds of

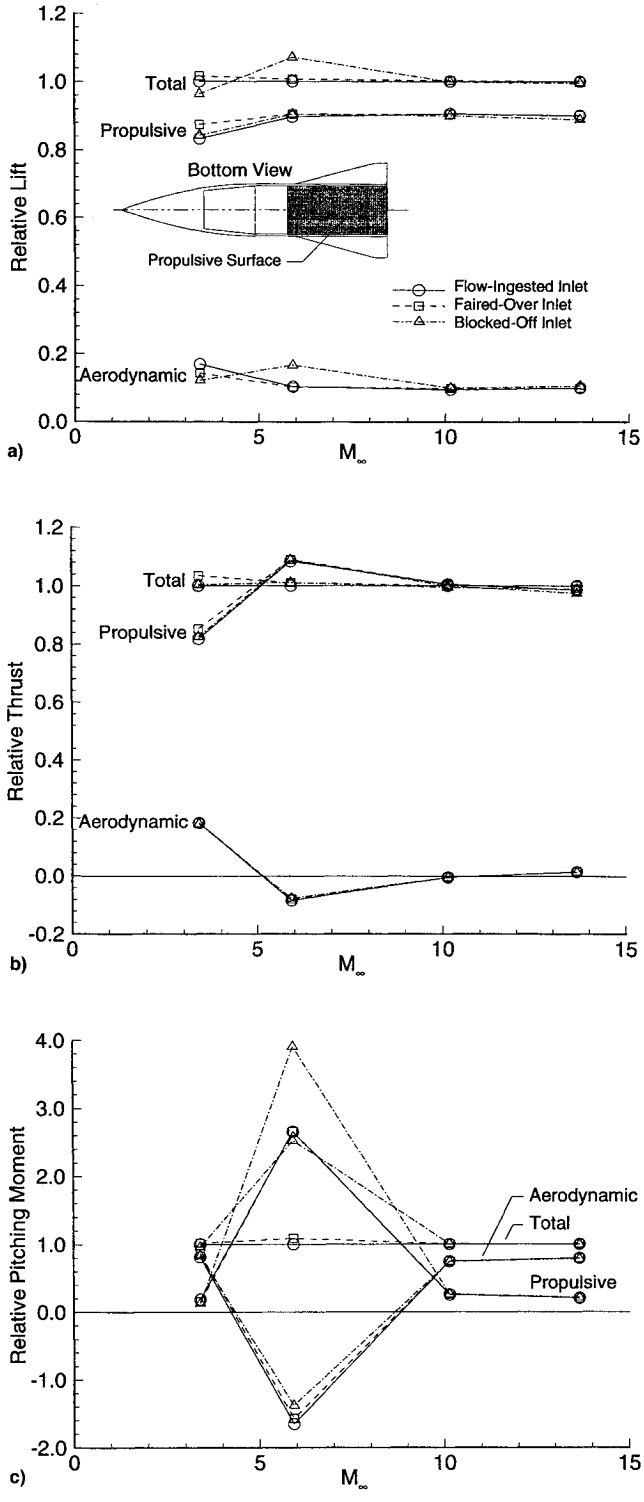

Fig. 7 Aftbody relative force and moment comparisons for flow-ingested and closed-inlet configurations: a) relative lift, b) relative thrust, and c) relative pitching moment.

information, the effect of inlet fairing throughout the Mach number range of interest and the contributions of the aerodynamic and propulsive surfaces on the aftbody. The shaded area in the TTD sketch on Fig. 7a defines the extent of the propulsive surface. The aerodynamic surface is the remainder of the aftbody, including the upper surface, wings, and aftbody sidewalls. Each of the three force and moment components presented has been nondimensionalized by their respective total aftbody force or moment value from the flow-ingested inlet solutions at the appropriate freestream Mach number. Thus, the total relative force and moment values for the flow-ingested inlet cases are unity.

Figure 7a shows relative lift on the aftbody as a function of freestream Mach number. In terms of the fairing effects, the faired-over inlet solution provides total lift values that are closer to the flow-ingested inlet solution at the two lower Mach numbers. At higher Mach numbers, the differences are negligible. Furthermore, the propulsive surface provides most of the contribution to the total lift on the aftbody at all Mach numbers. In terms of aftbody relative thrust (Fig. 7b), the overall differences of the two closed-inlet solutions are small compared to the flow-ingested inlet solution, with the blocked-inlet case showing slightly better agreement at the lower Mach numbers. As expected, the propulsive surface provides most of the aftbody thrust. Figure 7c shows the relative pitching moment on the aftbody for the three forebody configurations of interest. The faired-over inlet case compares very well with the flow-ingested inlet case throughout the Mach number range. The large discrepancy in the blocked-off inlet case at $M_\infty = 5.92$ is due in part to the larger lift predicted there (see Fig. 7a). Aside from the $M_\infty = 5.92$ condition, most of the pitching moment contribution is from the aerodynamic surfaces. Furthermore, these relative changes in pitching moment with increasing freestream Mach number are not trivial and not linear or smooth. In the region between $M_\infty = 4$ and $M_\infty = 8$, the external nozzle transitions from being highly overexpanded to highly underexpanded and causes large shifts in relative aerodynamic and propulsive forces and moments even without a fairing.

Based on comparisons of three-dimensional flowfield and aftbody force and moment data, the computational solutions presented show that, for the most part, either closed-inlet configuration may be satisfactory for determining downstream plume influences on powered-simulation models with metric aftbodies. If the entire model was metric, the cowl influences might be hard to separate and scale with Reynolds number on the blocked-off inlet case. As was seen two dimensionally,[11] the plume tends to isolate the aftbody surface from the forebody flowfield differences. Those configurations that employ a soft fairing were shown to provide aftbody surface characteristics that are nearly identical with a model representation that would ingest the inlet flow. Thus, a faired-over inlet is a viable solution to one of the problems of small-scale hypersonic powered testing of airbreathing vehicles.

Plume Characterization Results

In this section, the variation in plume extent will be presented for the flow-ingested (realistic) and faired-over inlet configurations. The wing impact of plume expansion will be discussed. Figure 8 compares the plume boundaries for the flow-ingested and faired-over inlet configurations at two locations on the aftbody for the four Mach numbers of interest. Contour levels are drawn for 5-, 25-, 50-, 75-, and 95% exhaust mass fractions. Midway down the aftbody (Fig. 8a), plume development has been established, and small differences appear in comparing the two configurations. More importantly, the extent of the plume/body intersection is seen to be quite dependent on the physical conditions. For instance, at $M_\infty = 3.40$, NPR = 30, the plume remains completely on the external nozzle surface, whereas the $M_\infty = 13.66$, NPR = 40,000 solutions definitely show plume impingement on the wing. These trends continue downstream, as shown by the comparisons at the body trailing edge (Fig. 8b). The $M_\infty = 3.40$ plume is still confined to the aftbody lower surface and the $M_\infty = 13.66$ plume completely bathes the lower surface of the wing. The vertical extent of the plume boundaries is slightly less for the flow-ingested inlet cases, but the lateral and model-proximity characteristics are nearly identical. Furthermore, the faired-over inlet configuration flow yields a slightly larger plume than the flow-ingested inlet configuration at the end of the body.

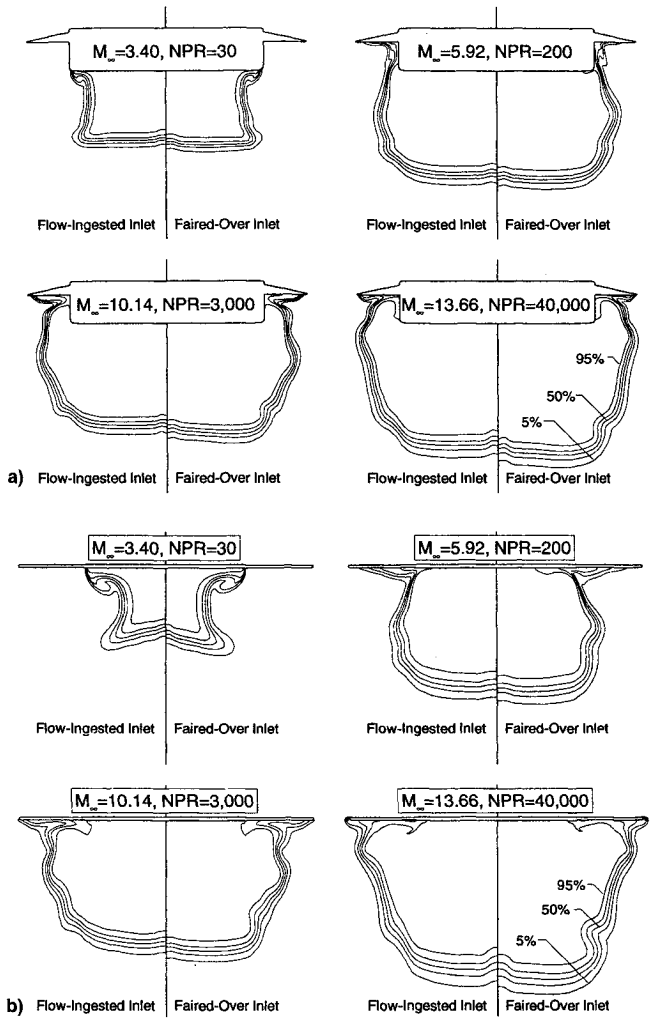

Fig. 8 Exhaust mass fraction contours, flow-ingested vs faired-over inlet configurations: a) midway down aftbody and b) body trailing edge.

Summary

Two studies have been presented addressing the computational capabilities of predicting complex three-dimensional hypersonic configuration flowfields under simulated powered conditions. Using a state-of-the-art CFD code, a three-dimensional inlet representation study was performed that showed that a faired-over or blocked-off inlet causes only minor differences as compared to a flow-ingested inlet in terms of the aftbody flowfield near the surface, aftbody surface pressures, and aftbody lift, thrust, and pitching moment. This indicates that the exhaust plume tends to isolate the aftbody surface from most of the forebody-generated flowfield differences. Thus, this type of technique, when applied to hypersonic wind-tunnel model testing under simulated powered conditions, can provide relatively accurate aftbody force and moment results. Finally, results of the plume characterization for these types of powered flows show a dramatic effect of plume expansion onto wing surfaces as the Mach number/NPR conditions are increased.

References

[1]Walters, R. W., Slack, D. C., Cinnella, P., Applebaum, M., and Frost, C., *A User's Guide to GASP, Revision 0*, Virginia Polytechnic Inst. and State Univ., Dept. of Aerospace and Ocean Engineering, and NASA Langley Research Center, Nov. 1990.

[2]McGrory, W. D., Huebner, L. D., Slack, D. C., and Walters, R. W., "Development and Application of GASP 2.0," AIAA Paper 92-5067, Dec. 1992.

[3]Huebner, L. D., Pittman, J. L., and Dilley, A. D., "Hypersonic Parabolized Navier-Stokes Code Validation on a Sharp-Nose Cone," *Journal of Aircraft*, Vol. 26, No. 7, 1989, pp. 650–656.

[4]Huebner, L. D., and Haynes, D. A., "Forebody Redesign and Flow Characterization of Test Technique Demonstrator at Mach 6," NASP TP-1013, April 1994.

[5]Huebner, L. D., "Computational Investigation of the LaRC Test Technique Demonstrator Reentry Configurations," *Seventh National Aero-Space Plane Technology Symposium* (Cleveland, OH), Vol. I, NASP CP-7040, 1989, pp. 153–174 (Paper 36).

[6]Huebner, L. D., and Tatum, K. E., "Computational and Experimental Aftbody Flowfields for Hypersonic, Air-Breathing Configurations with Scramjet Exhaust Flow Simulation," AIAA Paper 91-1709, June 1991.

[7]Tatum, K. E., Monta, W. J., Witte, D. W., and Walters, R. W., "Analysis of Generic Scramjet External Nozzle Flowfields Employing Simulant Gases," AIAA Paper 90-5242, Oct. 1990.

[8]Huebner, L. D., and Tatum, K. E., "CFD Code Calibration and Inlet-Fairing Effects on a 3D Hypersonic Powered-Simulation Model," AIAA Paper 93-3041, July 1993.

[9]Witte, D. W., Huebner, L. D., and Haynes, D. A., "Test Technique for Using Metric Model Parts to Obtain Powered Effects on Air-Breathing Configurations in Hypersonic Facilities," NASP TP-1008, Oct. 1993.

[10]Richardson, P. F., Parlette, E. B., Morrison, J. H., Switzer, G. F., and Dilley, A. D., "Comparison Between Experimental and Numerical Results for a Research Hypersonic Aircraft," *Journal of Aircraft*, Vol. 27, No. 4, 1990, pp. 300–305.

[11]Huebner, L. D., and Tatum, K. E., "Computational Effects of Inlet Representation on Powered Hypersonic, Air-Breathing Models," *Journal of Aircraft*, Vol. 30, No. 5, 1993, pp. 571–577.